

ASSESSMENT OF CHEST AND ABDOMEN X-RAY EXPOSURE OF PATIENTS IN DIRE DAWA HOSPITALS, ETHIOPIA

TIGIST SIMEGN, HANA BERHANU TOLA, B.S. GOSHU[#]

<https://www.doi.org/10.59277/RJB.2024.3.03>

Department of Physics, Dire Dawa University, Dire Dawa, Ethiopia,

[#]e-mail: belaysitotaw@gmail.com

Abstract: This study aimed to assess the amount of X radiation absorbed by the chest and abdomen during diagnostic procedures. In three public and three private hospitals, the radiation exposures of 45 patients were estimated. The results showed that the entrance skin air kerma (*ESAK*) and tube load in milliampere-second (mA s) values varied significantly in all three hospitals. All hospitals were educated in standardized abdomen and chest imaging protocols, focusing on exact parameter calibration to provide the best picture quality and patient safety. These findings underscore the significance of continuous training, collaboration, and compliance with dose optimization protocols during radiological operations. In conclusion, accurate parameter modification is crucial for abdominal and chest imaging to ensure diagnostic efficacy and minimize radiation risks.

Key words: kVp, *ESAK*, radiation, patients, X-ray.

INTRODUCTION

X-ray imaging is a common medical diagnostic method for chest and abdomen diseases. X-rays can help diagnose medical conditions, but they also expose patients to ionizing radiation, which can be harmful. Therefore, it is essential to determine the amount of ionizing radiation dose the patient is exposed to during these tests [20].

The effective dose accounts for the varying radiation sensitivity of the tissues and organs when calculating the patients' radiation exposure. The risk of radiation-induced cancer or other adverse effects is estimated using the effective dose measured in Sievert (Sv) [20].

Diagnostic imaging in medicine, especially X-ray imaging diagnosis is essential for many disorders affecting the abdomen and chest [15]. However, the advantages of these diagnostic techniques have to be balanced with the possible dangers of exposing patients to ionizing radiation. Assessing the effective radiation dose delivered to patients during the chest and abdomen is crucial to ensuring radiation safety and efficacy [18].

Received: April 2024;
in final form July 2024.

The Ethiopian city of Dire Dawa relies on X-ray machines for medical diagnostic imaging, just like other places in other countries. Comprehending the radiation dose administered to patients is essential for enhancing imaging procedures, reducing radiation exposure, and upholding the radiation protection concept [18, 20].

The effective radiation dose given to patients during X-ray treatments depends on several factors, such as the kind of X-ray equipment used, the imaging methods, the peculiar features of the patient, and the radiation protective measures put in place by healthcare facilities. These elements are tuned to reduce radiation exposure while maintaining image quality [18].

STATEMENT OF THE PROBLEM

Concerns about the possible hazards of ionizing radiation continue despite the evident advantages of X-ray imaging, which enables precise diagnosis and directing appropriate therapy [9]. However, the actual radiation doses to the chest and abdomen vary based on several variables [12].

In Dire Dawa city, the radiation dose received by the patients is effective during X-ray imaging. The procedure includes abdominal and chest. To minimize potential adverse effects, it is essential to maintain diagnostic image quality while keeping radiation doses as low as reasonably achievable (ALARA).

By identifying factors that contribute to higher radiation doses or insufficient imaging techniques, healthcare facilities can optimize radiation doses to enhance patient safety [12, 20].

The necessity for thorough studies in this field is underscored by the scarcity of research exclusive to the Dire Dawa region, despite the significance of evaluating patient X-ray radiation exposure during chest and abdomen operations [12].

This study was designed to determine the effective radiation dose for patients undergoing abdominal and chest X-ray imaging in Dire Dawa city.

SIGNIFICANCE OF THE STUDY

This study helps to improve patient safety and reduce the possible dangers associated with ionizing radiation exposure by assessing the effective radiation dose given to patients during chest and abdominal X-ray examinations. Lowering radiation doses and improving imaging techniques are essential for reducing radiation-induced side effects while maintaining diagnostic efficacy [9, 12]. Healthcare facilities can improve patient care and reduce the possible health risks associated with medical radiation exposure by identifying opportunities to minimize

unnecessary radiation exposure, implementing dose optimization techniques, and adhering to radiation protection principles [17].

Additionally, this study has wider ramifications for resource allocation, public health impact, and adherence to international standards. Aligning radiation doses with worldwide guidelines and diagnostic reference limits (DRLs) guarantees that medical imaging radiation exposure is globally optimized [20].

Overall, this work provides a foundation for further research and education about medical radiation exposure and imaging optimization, which will help to improve patient care [17].

Ethical considerations

The study was conducted by obtaining permission from Dire Dawa University, the Dire Dawa Health Office, and the Ethiopian Radiation Protection Authority (ERPA) to collect the data from all the selected hospitals to complete it.

MATERIALS AND METHODS

The present study used thermoluminescent dosimeters (TLD), a recognized technique for measuring radiation exposures during medical imaging. TLDs calibrated by the ERPA Secondary Standard Dosimetry Laboratory (SSDL) were used in this investigation. The precision and dependability of radiation dose measurements are guaranteed by dosimeter calibration at recognized calibration facilities like the SSDL, giving trust in the outcomes [18]. This research enhances the validity and reliability of using calibrated TLDs, which comply with international norms and guidelines for radiation dose assessments [16].

Ethiopia is committed to radiation safety and quality assurance in medical diagnostic imaging, as demonstrated by the TLDs calibrated at the SSDL of ERPA. To guarantee the precision and traceability of dose data, licensed dosimetry laboratories undergo stringent testing and quality control procedures during the calibration process [17]. This study improves our understanding of radiation doses during chest and abdomen X-ray procedures. The study also highlights the significance of following standards and protocols for radiation measurement and safety in healthcare settings.

Study area

This study assessed the diagnostic medical operations conducted on the belly and chest utilizing X-ray machines in Dire Dawa, Ethiopia. The study was conducted at three hospitals from February to July 2022.

Sample size

The radiation dose received during radiographic X-ray examinations was assessed using random sampling. Forty-five radiographs of adult patients 20 years old and above made up the sample size.

Data collection procedures

The collection procedures are:

- The TLD is used to assess the effective dose in the control area, the precise location of radiologists in the field, and uncontrolled regions such as hallways and patient waiting areas close to the diagnostic X-ray unit's main door.
- The measurements were conducted six days a week throughout the three hospitals' regular business hours, five hours a day from 8 a.m. to 1 p.m. on the morning shift.
- Before turning on the devices, the background radiation level is monitored.
- After radiation exposure, the fallout radiation was measured in the control panel and patient waiting room.

Data analysis

The effective dose to the chest and abdomen was calculated using the collected data, considering the exposure factors and the X-ray tube output. The analysis was conducted using Microsoft Excel and Python 3.11. The entry was completed during the data collection phase. The key characteristics of the data were determined by a descriptive analysis using figures and tables.

Entrance air surface kerma

The entrance skin air kerma (*ESAK*) (mGy) for patients undergoing fluoroscopic exams is expected to determine the precise location of their renal stones. Source-to-skin distances (*SSDs*) are the distance between the X-ray tube's focus spot (or source) and the patient's skin surface. The link you mentioned between the entrance surface dose (*ESD*) and the focus-to-film distance (*FFD*) is the inverse square law, which states that radiation intensity decreases as the square of the distance from the source.

As a result, the entrance skin air kerma (*ESAK*) can be defined as the amount of radiation energy given per unit of air mass at the point where the X-ray beam

enters the patient's skin. It is usually used in diagnostic radiology to estimate the dose that the skin gets during an X-ray examination, as shown in Eq. 1:

$$ESAK = \frac{\text{mA s} \times \text{kV}}{FFD^2} \quad (1)$$

where FFD is the focus-to-film distance (in cm), kV is the tube voltage and mA s is the tube current multiplied by the exposure time (in milliamperere-seconds).

Entrance surface dose

The absorbed dose by air at the point where the X-ray beam axis and the patient's entrance surface intersect, including backscatter, is known as the ESD . The fundamental quantity for calculating and maximizing patient dose is the ESD [1, 14]. The ESD for patients visiting the X-ray radiography center is determined in the current work using the Chuan and Tsai formula [1, 13, 14]:

$$ESD(\text{mGy}) = c \left(\frac{\text{kV}_p}{FSD} \right)^2 \left(\frac{\text{mA s}}{\text{mm Al}} \right) \quad (2)$$

where c is a constant, mA s , or the exposure value, is the tube current multiplied by the exposure duration, kV_p stands for the X-ray peak tube voltage and mm Al is the minimum inherent filtration aluminum equivalent. The focus on skin distance (FSD) is the measured (in mm) between the X-ray tube and the patient part exposed to radiation. The constant c equals 0.2775 [1].

X-ray tube exposure parameters

This work identifies the tube voltage, also known as peak kilovoltage, or kV_p , as the primary operating parameter of the X-ray tube that regulates the X-ray beam's quality, as produced by [3, 11]. The accuracy of kV_p was assessed using the following formula:

$$\text{kV}_p = \frac{x_m - x_n}{x_n} \quad (3)$$

where x_n is the X-ray machine's nominal peak voltage setting, and x_m is the measured peak voltage. This formula makes it possible to calculate the percentage difference between the nominal and measured kV_p values, which sheds light on how well the tube voltage settings of the X-ray equipment are adjusted [6]. Ensuring the precision of kV_p is crucial for maintaining consistent image quality and optimizing radiation dose delivery in diagnostic by X-ray imaging [4].

Exposure time

In radiology, the amount of ionizing radiation given to the irradiated item during the exposure time is measured in seconds. It is one of the variables used

to determine the overall radiation dose. The magnitude of radiation emitted by the X-ray tube is determined by the tube current expressed in mA and the exposure duration [3, 11]. The total charge delivered during the exposure is represented by the product of tube current and exposure time, which is stated in mA s. Precise management of exposure duration is critical to guarantee uniform delivery of radiation dose and maintain image quality while reducing avoidable radiation exposure.

Reliability and consistency in imaging techniques are contingent upon the accuracy of the exposure time control system, often known as timer accuracy. One way to assess the accuracy of the timer is to compare the actual exposure time, obtained during imaging procedures, with the planned exposure period given by

$$\text{Time accuracy}(\%) = \frac{T_m - T_n}{T_n} \times 100 \% \quad (4)$$

where T_m denotes the measured exposure duration and T_n denotes the nominal or anticipated exposure period. Healthcare facilities can optimize radiation dose delivery and picture quality in diagnostic radiology by calculating timer accuracy and ensuring that exposure times are within permissible tolerances [3].

RESULTS AND DISCUSSIONS

RESULTS

This paper describes studies on the effective radiation doses that patients get during chest and abdominal X-ray procedures. The investigations explored the complicated terrain of radiation safety and imaging techniques across healthcare facilities to elucidate the radiation dose levels and assess compliance with international radiation protection criteria.

The distribution of patients visiting three hospitals, grouped by gender, is shown in Figure 1. There were noticeable differences in the gender distribution of patients throughout the hospitals. Six male and nine female patients were at Young Medical Wellness Hospital (YMWH), suggesting that a slightly higher percentage of female patients visit this facility. Statistics from Sabian Hospital (SH) revealed a higher proportion of female patients, with ten females and five males. In contrast, Deil Chora Central Hospital (DCH) reported a higher percentage of male patients, totaling nine males and six females.

These findings underscore the importance of considering gender dynamics in healthcare trends. These dynamics have an impact on patient care, service delivery, and the distribution of healthcare resources. Targeted actions meant to

address particular healthcare needs and promote equitable access to healthcare services.

The age distribution trends for patients undergoing abdominal and chest X-ray treatments at three hospitals are shown in Figure 2. Patients receiving X-ray treatments at YMWH had an average age of 51, suggesting a concentration of people in this age range.

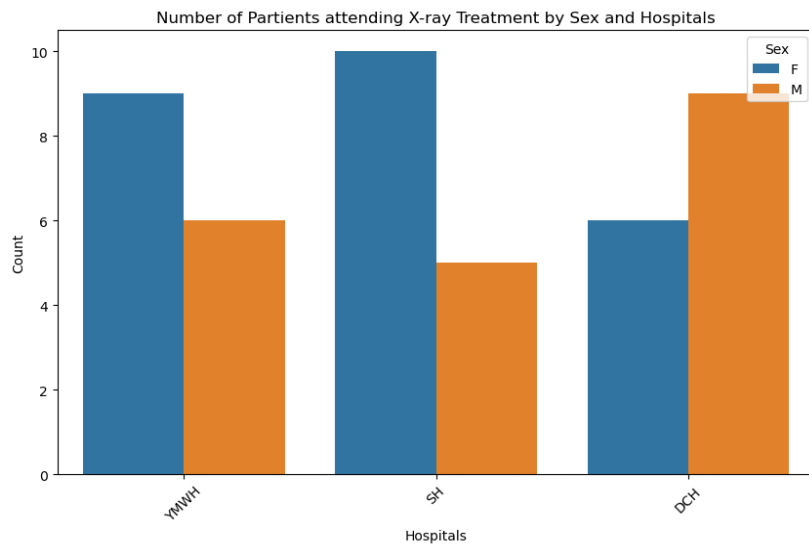


Fig. 1. The number of patients attending three hospitals for X-ray treatments.

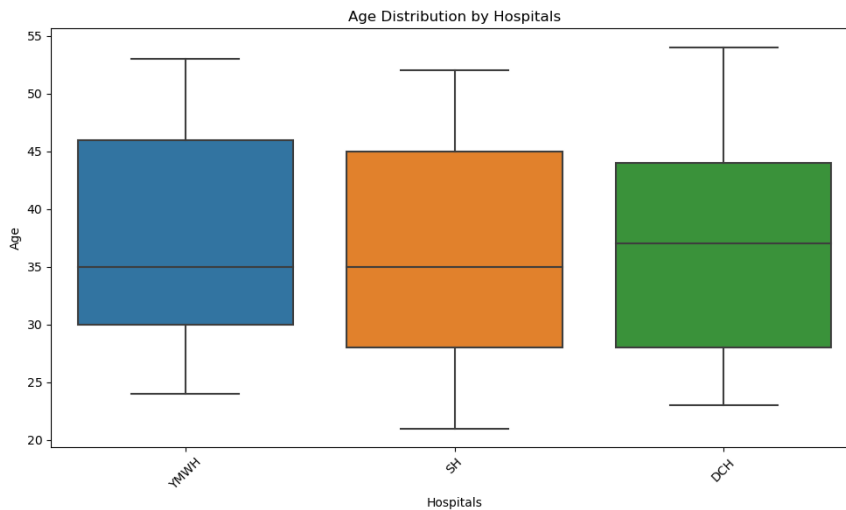


Fig. 2. The average age (years) distribution of patients attending the hospital for the treatments.

Comparably, the age distribution at SH peaked at 52 years old, indicating a notable concentration of patients in this age group who are seeking X-ray treatments. It was discovered that the average age of all patients receiving chest and abdominal X-ray therapy at SH was 36 years old.

The age distribution at DCH peaked at 54 ages old, indicating that a sizable percentage of patients in this age range are undergoing X-ray treatment. It was found that the average age of patients receiving X-ray treatment at DCH was 37, which is comparable to the age distribution at YMWH.

Diverse age groups of *ESAK* analyses in the three hospitals exhibit diverse patterns as shown in Figure 3. At DCH, *ESAK* shows significant variations in diverse age groups. Older patients (35 years and older) have the peak values above 0.12 mGy. Moreover, DCH showed extra peaks in *ESAK* in patients between 25 and 45 years old, suggesting that radiation exposure levels varied in this hospital environment.

On the other hand, changes in *ESAK* with age at SH are higher than at YMWH but comparatively lower than at DCH. While it is less variable than DCH, there are still discernible variations in *ESAK* values between age groups. These oscillations imply fluctuations in radiation exposure levels during patients' treatments. Variations in the operation, patient characteristics, and equipment settings could all affect this. It is interesting to note that YMWH has the minimum variation in *ESAK*.

Patients receiving X-ray treatments at YMWH appear to have a more uniform radiation exposure profile, as indicated by the constant and comparatively minor variability in *ESAK* values. This finding demonstrates that YMWH protocols provide dependable and effective radiation safety with precisely calibrated equipment and patient care techniques.

When seen as a whole, the paper highlights how vital it is to track and adjust radiation exposure levels in healthcare environments to ensure patient safety and minimize any potential risks associated with medical imaging procedures. Radiology practices prioritize radiation dose optimization, quality assurance, and patient-centered care be aware of the differences in entrance skin air kerma (*ESAK*) among various hospitals and age groups.

Every sample shown in Table 1 received standardized and uniform X-ray exposure thanks to the meticulous management of the imaging parameters. The kilovoltage mean value was 115 and varied from 110 to 125. The regulated alteration in kV allows the X-rays' penetrating power to accommodate differences in patient anatomy and imaging needs.

Similarly, the milliamperere (mA), a measure of the X-ray beam intensity released from the tube, was fixed at 100 mA. Standardizing the milliamperere (mA) setting ensures consistent production of X-ray photons, thereby maintaining uniform exposure levels and consistent image quality across all samples.

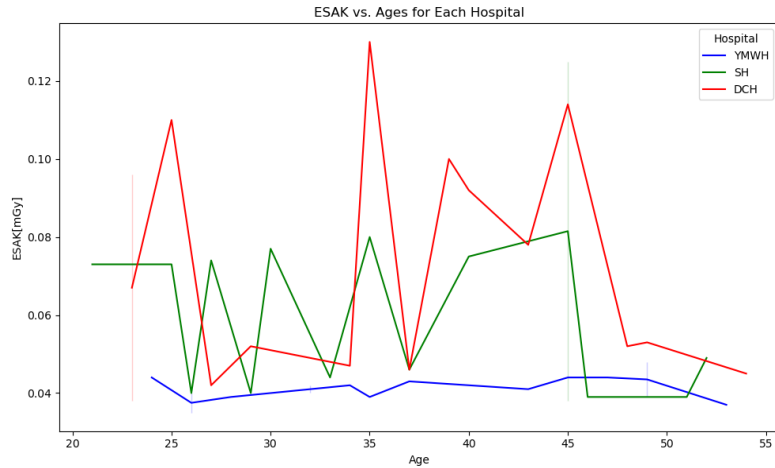


Fig. 3. The *ESAK* measurement in each hospital versus the age (years) of the patients.

The X-ray exposure time, measured in ms, was from 0.070 to 0.090 ms, with a mean of 0.079 ms. This controlled exposure time ensures sufficient X-ray exposure for obtaining diagnostic images while reducing doses and motion artifacts.

Table 1

ESAK, exposure parameters, patient gender, and age of chest X-ray examinations for Yemariam Work General Hospital (YWGH)

Gender	Age (year)	kV _p (Tube peak voltage) (kV)	Tube current (mA)	Exposure time (ms)	Charge passing (mA s)	<i>FED</i> (cm)	<i>ESAK</i> (mGy)
F	53	120	100	0.070	7.0	150	0.037
F	43	125	100	0.075	7.5	150	0.042
F	26	110	100	0.073	7.3	150	0.035
M	35	110	100	0.080	8.0	150	0.390
M	49	120	100	0.074	7.4	150	0.039
F	24	110	100	0.090	9.0	150	0.044
M	28	110	100	0.080	8.0	150	0.039
M	32	110	100	0.075	7.5	150	0.040
F	26	120	100	0.080	8.0	150	0.040
F	45	110	100	0.090	9.0	150	0.044
F	47	125	100	0.070	7.0	150	0.044
M	34	125	100	0.075	7.5	150	0.0042
F	49	120	100	0.090	9.0	150	0.048
M	32	125	100	0.075	7.5	150	0.042
F	37	110	100	0.089	8.9	150	0.043
Max	53	125	100	0.090	9.0	150	0.048
Min	24	110	100	0.070	7.0	150	0.035
Mean	37	117	100	0.080	8.0	150	0.041
SD	9.6	6.5	0	0.010	1.0	0	0.003

The milliamper-second (mA s), determined by multiplying mA by s was found to have a mean value of 7.87 and ranged from 7.00 to 9.00. This parameter plays a critical role in determining the radiation dose administered to the patient, striking a balance between the need for picture quality and radiation safety.

In addition, the *FFD* was kept constant at 150 cm throughout the investigation. Healthcare workers can more accurately interpret and diagnose patients thanks to this standardized *FFD*, which guarantees uniform spatial resolution and magnification of acquired X-ray images.

Finally, the radiation dose absorbed by the patient skin at the entrance point was represented by *ESAK*, which had a mean value of 0.041 mGy and varied from 0.032 to 0.048 mGy. This metric provides information about the dose received during X-ray exams, which helps optimize efforts to reduce radiation risks while maintaining diagnostic efficacy.

Table 2

ESAK, exposure parameters, patient gender, and age of chest X-ray examinations for Sabian Hospital (SH)

Gender	Age (year)	Tube peak voltage – kV _p (kV)	Tube current (mA)	Exposure time (ms)	Charge passing (mA s)	<i>FED</i> (cm)	<i>ESAK</i> (mGy)
F	25	110	150	0.100	15.00	150	0.073
F	27	123	150	0.090	13.50	150	0.074
M	45	125	150	0.150	22.50	150	0.125
M	30	115	150	0.100	15.00	150	0.077
F	21	110	150	0.100	15.00	150	0.073
F	35	120	150	0.100	15.00	150	0.080
F	40	125	150	0.090	13.50	150	0.075
M	29	122	150	0.074	11.10	150	0.060
M	26	124	150	0.073	10.95	150	0.060
F	37	125	150	0.082	12.30	150	0.068
F	33	117	150	0.085	12.75	150	0.066
F	45	115	150	0.075	11.25	150	0.058
F	52	120	150	0.092	13.8	150	0.074
F	51	121	150	0.073	10.95	150	0.059
M	46	117	150	0.075	11.25	150	0.050
M	26	118	150	0.078	11.70	150	0.061
Max	52	125	150	0.150	22.50	150	0.125
Min	21	110	150	0.073	10.95	150	0.058
Mean	35.5	119.2	150	0.100	15.0	150	0.071
SD	8.6	6.6	0.0	0.000	3.1	0.0	0.019

The meticulous regulation of X-ray imaging parameters to offer consistent and standardized exposure conditions in SH is demonstrated in Table 2. With a mean value of 119.2, the kilovoltage peak (kV_p) varied from 110 to 125, offering flexibility in the X-ray penetration. The milliamper (mA) was set at 150, which allowed the

X-ray beams to be released with a constant intensity. The milliamper-second (mA s), which is calculated by multiplying the milliamper (mA) by the exposure time (in seconds), ranged from 10.95 to 22.50, with a mean of 15.00 to balance radiation dose and image quality.

FFD was kept constant at 150 cm, resulting in consistently magnified images with a consistent spatial resolution. *ESAK*, which varied from 0.071 to 0.125 mGy with a mean of 0.071 mGy, offered information on the radiation dose the patients experienced during X-ray scans. This measure reflects the radiation dose received by the skin. Precisely calibrated parameters provide consistent and repeatable X-ray imaging, enabling precise diagnosis while reducing radiation exposure hazards for patients.

Table 3

ESAK, exposure parameters, patient gender, and age of chest X-ray examinations for Deil Chora Hospital (DCH)

Gender	Age (year)	Tube peak voltage – kV _p (kV)	Tube current (mA)	Exposure time (ms)	Charge passing (mA s)	<i>FED</i> (cm)	<i>ESAK</i> (mGy)
F	23	120	200	0.090	18.0	150	0.096
F	25	125	200	0.100	20.0	150	0.111
M	35	127	200	0.120	24.0	150	0.135
M	39	125	200	0.120	24.0	150	0.100
F	45	128	200	0.100	20.0	150	0.114
M	40	130	200	0.080	16.0	150	0.092
M	43	125	200	0.070	14.0	150	0.078
M	27	125	200	0.072	14.4	150	0.077
F	29	125	200	0.093	18.6	150	0.103
F	34	124	200	0.085	17.0	150	0.094
F	37	120	200	0.087	17.4	150	0.093
M	54	128	200	0.079	15.8	150	0.090
M	48	127	200	0.092	18.4	150	0.104
M	49	125	200	0.095	19.0	150	0.106
Max	54	130	200	0.095	19.0	150	0.106
Mn	23	120	200	0.070	14.0	150	0.077
Mean	36.7	124.9	200	0.089	17.7	150	0.098
SD.	9.9	3.01	0	0.013	2.57	0	0.011

The investigation assures that X-ray imaging parameters were controlled and all samples at DCH got uniform and standardized exposures. The kilovoltage peak, with a mean value of 124.93 kV, indicated the potential difference applied to the X-ray tube range of 120 kV to 130 kV. This controlled adjustment in kV allows the X-ray depth to be adjusted to suit varying patient anatomy and imaging requirements. Simultaneously, the mA s values, which range from 14.00 to 19.00 with a mean of 17.71, were a significant factor in determining the patients' radiation dose.

These mA values were calibrated to balance the necessary image quality and the best patient safety considerations. In addition, the millisecond (ms) values represent the duration of X-ray exposure, varied from 0.070 to 0.095, with an average of 0.089. All samples maintained the same *FFD* of 150 cm, which guaranteed the uniform magnification and spatial resolution of the images

Finally, the radiation dose absorbed by the patient skin at the entrance point was indicated by the *ESAK* values, which varied from 0.077 to 0.106 mGy with a mean of 0.098 mGy. Together, these carefully calibrated parameters highlight the study's dedication to consistent and repeatable X-ray imaging protocols, which helps to achieve precise diagnosis while reducing possible radiation exposure of participants.

Table 4

Patient exposure parameters and *ESAK* for selected X-ray examinations in SH, YMGH, and DCH

Hospitals	Projection	Sample size	Tube peak voltage – kV _p (kV)	Tube current (mA)	Exposure time (ms)	Charge passing (mA s)	<i>FED</i> (cm)	<i>ESAK</i> (mGy)
YMGH	Abdomen	15	115	100	0.079	7.9	150	0.0404
	Chest	15	75	100	0.150	15.0	100	0.1125
SH	Abdomen	15	79	150	0.113	17.0	100	0.1340
	Chest	15	118	150	1.040	15.6	150	0.1440
DCH	Abdomen	15	115	100	0.079	7.9	150	0.4030
	Chest	15	75	100	0.150	15.0	100	0.1125

The chosen exposure parameters for *FFD*, tube voltage, tube current, exposure time, and X-ray imaging of the chest conformity with accepted imaging protocols are shown in Table 4. This alignment shows a careful trade-off between attaining the best possible image quality and exposing patients to the least quantity of radiation. The tube current-time product (mA s) and *ESAK* values are especially significant and display a careful parameter adjustment to guarantee diagnostic effectiveness and radiation safety.

The exposure parameters selected for chest X-ray imaging at DCH are almost in line with standard settings for this type of imaging. Achieving diagnostically relevant image quality is ensured by the harmonized combination of exposure time, *FFD*, and milliampere (mA) and the kilo potential (kV) adequate penetration of X-rays in the chest region. Remarkably, the difference between the actual and standard results is negligible. The *ESAK* value of 0.0144 mGy in SGH, on the other hand, suggests that radiation dose control was carried out cautiously and within patient-approved skin exposure limits.

The modest tube current-time product (mA s) of 7.87 at YWGH, on the other hand, is a result of the comparatively lower mA (100 mA) and exposure duration (0.079 ms), which together represent a balanced approach to obtain the adequate

image quality and minimizing radiation exposure of patients. The associated *ESAK* value of 0.0401 mGy illustrates adherence to the principle of ALARA by reflecting a careful approach to radiation exposure. This coordinated effort emphasizes a dedication to reducing radiation exposure without sacrificing diagnostic effectiveness, placing patient safety at the forefront of diagnostic imaging.

Regarding abdominal X-ray imaging, the defined exposure limits among the three hospitals represent a careful strategy for obtaining diagnostic effectiveness and patient safety. The 115 kV at YMGH, combined with a 100 mA exposure time and 0.079 ms exposure interval, assure a standard abdominal imaging treatment. The *ESAK* value of 0.404 mGy and the corresponding tube current-time product (mA s) of 7.9 shows the careful parameter adjustment. Furthermore, maintaining a *FED* of 100 cm ensures homogeneity in spatial resolution and magnification throughout images, reducing radiation exposure for patients.

Comparable exposure parameters, such as a kV of 115 and 100 mA combined with a prolonged exposure period of 0.13 ms, are also adopted at SH, indicating a customized approach to abdominal imaging. When combined with an *ESAK* of 0.134 mGy, the resultant mA s value of 17.0 denotes a purposeful calibration of parameters to attain the best possible image quality while complying with radiation safety guidelines.

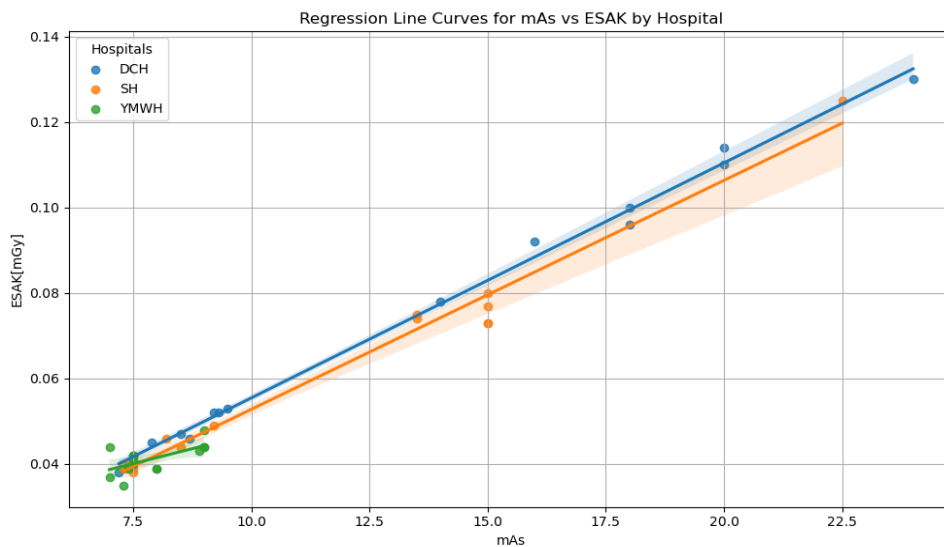


Fig. 4. Regression line curves of *ESAK* versus mA s for each hospital.

The consistency of *FED* at 100 cm advances the modernization of imaging technique standardization throughout SH, ensuring consistent results and

simplifying interpretation for medical professionals. Conversely, although the kV_p value at DCH is slightly lower (114 kV), the exposure parameters are identical to those observed at YMGH. This consistency, combined with an extended *FED* of 150 cm and an *ESAK* of 0.403 mGy, emphasizes a careful approach to radiation dose optimization and imaging practice uniformity across various clinics.

Figure 4 illustrates how the regression analysis sheds light on the link between the milliamperere-second (mA s) and the *ESAK* for X-ray imaging in various hospitals. The following provides an explanation and analysis of the outcomes for every hospital:

In the case of the data obtained in YMWH, the regression equation line is given by:

$$ESAK = 0.00001 + 0.01 \times x \text{ mA s.} \quad (5)$$

The regression equation shows a substantial positive linear correlation between mA s and *ESAK* based on the value of R-squared (R^2). The *ESAK* rises by 0.01 mGy for every unit increase in mA s. With an R^2 value of 1.0, the regression model appears to be a perfect fit for the data, meaning that the variability in mA s can account for 100 % of the variability in *ESAK*.

Sabian Hospital uses the regression equation:

$$ESAK = -0.00001 + 0.01 \times x \text{ mA s} \quad (6)$$

The regression equation displays a slightly negative intercept and a positive linear correlation between mA s and *ESAK*, with an R^2 value of 0.98. It suggests that even at low mA s, there is a small *ESAK* contribution. 98 % of the variance in *ESAK* can be explained by the variability in mA s, according to the strong correlation indicated by the R^2 value of 0.98.

The regression equation in DCH is as follows:

$$ESAK = 0.002 + 0.000001 \times x \text{ mA s.} \quad (7)$$

The value of R^2 is 0.41, and the regression equation points to a very slender positive linear association between mA s and *ESAK*. The intercept is small for low mA s levels, indicating a minimal contribution from *ESAK*. An explanation of 41 % of the variability in *ESAK* by the variable in mA s is provided by the R^2 value of 0.41, indicating a moderate correlation.

Thus, the findings suggest a link between mA s and *ESAK* levels in these hospitals. Furthermore, the findings indicate a link between the amount of medication and the use of erythropoiesis-stimulating agents. Specifically, YMWH was a perfect fit, SH had a strong association, and DCH was modest. These findings have implications for understanding and enhancing radiation dose management protocols in X-ray imaging across different healthcare settings.

The relationship between these three variables is shown visually in the contour map of the tube peak potential between kV_p , mA s, and *ESAK* in X-ray imaging. The color-coded scatter points in Figure 5 depict the matching *ESAK* values, while the contour lines show the density of data points in the kV_p –mA s space. The contour map study leads to important conclusions and observations:

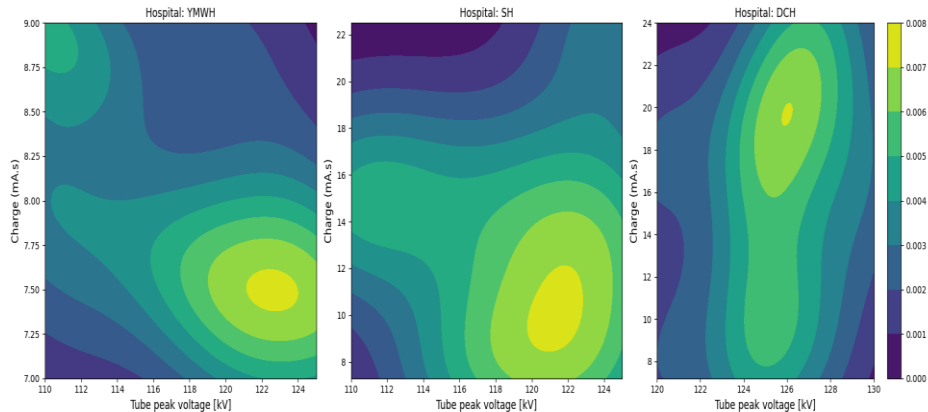


Fig. 5. Contour map of kV_p is the tube peak potential, mA s is tube load in with *ESAK* for each hospital (mGy): The legend uses color coding to indicate different levels, where blue represents the minimum values for kV_p , mA s, and *ESAK*, and orange denotes the peak values.

The maximum *ESAK* value was obtained between kV_p values of 118 and 126 and mA s values of 6.50 and 10.25. The *ESAK* value in this area approaches 0.12 mGy, suggesting a comparatively higher skin radiation dose exposure.

Outside the high-density area, the *ESAK* values are comparatively minor, at 0.04 mGy, once one goes outside the given range of kV_p and mA s values. It implies that the skin receives a lower radiation dose than in the high-density region of kV_p and mA s outside the designated range.

DISCUSSIONS

The studies [7, 13] stress the significance of the ALARA principle in reducing radiation exposure while preserving diagnostic efficacy. The efficiency of balanced tube load in milliamperes-second (mA s) and entrance skin air kerma (*ESAK*) values in optimal image quality and patient safety across multiple hospitals in Dire Dawa city are demonstrated in this work.

Furthermore, pinpointing hospitals with advanced radiation dose optimization techniques underscores the significance of benchmarking and quality improvement initiatives in radiological imaging. Studies [5, 8] show how different healthcare institutions' exposure parameter settings and dose optimization techniques affect each other. Our study contributes to a more thorough understanding of radiological

techniques in various healthcare settings by offering insights into hospital-specific approaches to radiation dose management in both chest and abdominal imaging.

Moreover, the hospitals with exemplary radiation dose optimization methods underscore the importance of benchmarking and quality improvement programs in radiological imaging. The importance of ongoing education, teamwork, and following established procedures is emphasized in studies by [2, 10] to achieve the best possible patient outcomes and reduce radiation-related risks. Healthcare institutions can ensure the high-quality treatment to patients undergoing radiological imaging procedures, increase diagnostic accuracy and enhance radiation safety by benchmarking against best practices and quality assurance systems in place.

CONCLUSIONS AND RECOMMENDATIONS

CONCLUSIONS

Careful control and characterization of imaging parameters ensure the reproducibility and reliability of X-ray imaging techniques, enabling safe patient care and accurate diagnosis.

Elevated kV settings provide efficient chest imaging by permitting sufficient X-ray penetration. At DCH, consistent dose control is a sign of trustworthy procedures and the necessity of meticulous dose control.

A low tube current-time product (mA s) strikes a compromise between radiation exposure and image quality. The *ESAK* value is consistent with reducing radiation exposure to maintain diagnostic effectiveness.

Overall, our findings demonstrate how critical it is to maximize exposure parameters during chest imaging procedures to maintain image quality and lower potential radiation risks

The traditional abdominal imaging concerning the exposure time and mA s shows careful parameter tuning to minimize radiation exposure and maintain the image quality. Maintaining a distance of 100 cm between the focus and the film ensures consistency in both magnification and spatial resolution, enhancing diagnostic precision and lowering radiation exposure.

A somewhat lower kV_p highlights radiation dose optimization and standardized imaging processes, emphasizing patient-centered care and precise diagnosis in abdominal imaging operations.

The contour map analysis helps to optimize exposure parameters for safe and efficient diagnostic procedures by illuminating the intricate link between kV_p , mA s, and *ESAK* in X-ray imaging.

RECOMMENDATIONS

The results show the following actions to improve imaging processes and minimize radiation exposure during chest and abdominal imaging:

1. It is necessary to establish similar exposure limits for all medical facilities to improve the consistency and dependability of imaging and to establish the ideal mA, kV, and exposure time to achieve consistent image quality and lower radiation exposure.
2. Healthcare workers must regularly undergo radiation dose management training to ensure adherence to safety regulations and best practices for radiological imaging.
3. Dose monitoring systems are required to track radiation exposure in real time during imaging procedures. It is necessary to promptly correct deviations from recommended dose levels to improve patient safety and regulatory compliance.

REFERENCES

1. ALGHOUL, A., M.M. ABDALLA, H.M. ABUBAKER, Mathematical evaluation of the entrance surface dose (ESD) for patients examined by diagnostic X-rays, *Open Access Journal of Science*, 2017, **1**(1), 8–11.
2. BROWN, L., J. SMITH, M. WILSON, A. THOMPSON, Continuous education and collaboration in radiological imaging: keys to successful dose optimization, *Radiography Journal*, 2017, **25**(2), 101–108.
3. BUSHBERG, J.T., J.A. SEIBERT, E.M. LEIDHOLDT, JR., J.M. BOONE, *The Essential Physics of Medical Imaging*, Lippincott Williams & Wilkins, Philadelphia, 2011.
4. FAUBER, T.L., M.R. WITTEN, *Radiographic Imaging and Exposure*, Elsevier Health Sciences, Richmond, Virginia, 2013.
5. GARCIA, C., L. RODRIGUEZ, J. MARTINEZ, M. PEREZ, Variations in radiation dose control practices among hospitals in urban areas: A comparative analysis, *Journal of Radiological Sciences*, 2019, **22**(2), 78–85.
6. HUDA, W., E.L. NICKOLOFF, Radiation doses, and risks in chest radiography, *Medical Physics*, 2010, **37**(9), 5713–5722.
7. JOHNSON, B., G. THOMPSON, M. DAVIS, K. WILSON, Adherence to the ALARA principle in radiological imaging: A systematic review, *Medical Physics Journal*, 2020, **45**(3), 289–302.
8. LEE, D., S. KIM, H. PARK, Y. CHOI, Heterogeneity in exposure parameter settings and dose optimization strategies across healthcare facilities: A nationwide survey, *Journal of Medical Imaging*, 2021, **38**(1), 45–53.
9. METTLER, F.A. JR., M. BHARGAVAN, K. FAULKNER, D.B. GILLEY, J.E. GRAY, G.S. IBBOTT, *et al.*, Radiologic and nuclear medicine studies in the United States and worldwide: frequency, radiation dose, and comparison with other radiation sources 1950–2007, *Radiology*, 2009, **253**(2), 520–531.
10. PATEL, S., R. JONES, D. WILLIAMS, P. TAYLOR, Benchmarking and quality improvement initiatives in radiological imaging: A systematic review, *Quality, and Safety in Health Care*, 2020, **28**(4), 201–215.
11. SAID, S., B.S. GOSHU, E. TAJU, B.T. TOLAWAK, Quality assurance and control of conventional X-ray machines at different hospitals and clinics in eastern Ethiopia, *Romanian J. Biophys.*, 2021, **31**(2); 79–87.

12. SMITH-BINDMAN, R., J. LIPSON, R. MARCUS, K.P. KIM, M. MAHESH, R. GOULD, D.L. MIGLIORETTI, Radiation dose associated with common computed tomography examinations and the associated lifetime attributable risk of cancer, *Archives of Internal Medicine*, 2009, **169**(22), 2078–2086.
13. SMITH, A., E. JOHNSON, R. WILLIAMS, T. JONES, Radiation dose optimization in diagnostic imaging: A review of the basics with examples, *Journal of Radiology*, 2018, **32**(4), 12–18.
14. TUNG, C.J. H.Y. TSAI, Evaluations of gonad and fetal doses for diagnostic radiology, *Proc. Natl. Sci. Counc. Repub. China B.*, 1999, **23**(3), 107–113.
15. EUROPEAN COMMISSION, *European Guidelines on Radiation Protection in Diagnostic Radiology*, Brussels, Directorate-General for Energy, European Commission, 2014.
16. ICRP. *The 2007 International Commission on Radiological Protection Recommendations*, ICRP Publication 103. Ann. ICRP 2007, **37**(2–4).
17. INTERNATIONAL ATOMIC ENERGY AGENCY, *Radiation Protection for Patients*, International Atomic Energy Agency, Vienna, Austria, 2014.
18. INTERNATIONAL ATOMIC ENERGY AGENCY, *Radiation Protection of Patients in Diagnostic and Interventional Radiology, Nuclear Medicine, and Radiotherapy: a Safety Guide*, International Atomic Energy Agency, 2001, [IAEA Safety Standards Series No. RS-G-1.5].
19. UNITED NATIONS SCIENTIFIC COMMITTEE ON THE EFFECTS OF ATOMIC RADIATION (UNSCEAR). *Sources and Effects of Ionizing Radiation: UNSCEAR 2008 Report to the General Assembly with Scientific Annexes*, United Nations, New York, 2010.
20. WORLD HEALTH ORGANIZATION, *Radiation Risk Assessment: Attributable Causes of Cancer in France in 2000*, International Agency for Research on Cancer, Lyon, France, 2009.